Detection of Thermal Aging Degradation and Plastic Strain Damage for Duplex Stainless Steel Using SQUID Sensor

M. OTAKA, S. EVANSON, K. HASEGAWA, K. TAKAKU
Hitachi Ltd., Hitachi, Japan

ABSTRACT

An apparatus using a SQUID sensor is developed for nondestructive inspection. The measurements are obtained with the SQUID sensor located approximately 150 mm from the specimen. The degradation of thermal aging and plastic strain for duplex stainless steel is successfully detected independently from the magnetic characterization measurements. The magnetic flux density under high polarizing field is found to be independent of thermal aging. Coercive force increases with thermal aging time. On the other hand, the magnetic flux density under high field increases with the plastic strain. Coercive force is found to be independent of the plastic strain.

1 INTRODUCTION

A SQUID (Superconducting Quantum Interference Device) sensor is an ultra-sensitive (typical resolution is 10^{-14}T) magnetic sensor which has been applied to biomagnetic measurements, geophysical measurements and so on.

In recent years, the SQUID sensor has formed the basis for several new techniques of magnetic NDE(Nondestructive Evaluation), for example detection of defects in carbon steel (Bain et al. (1987)) and the measurement of galvanic corrosion currents (Bellingham et al. (1987)). We have developed a detection system of damage in materials using the SQUID sensor.

In this paper, we report on the developed SQUID apparatus for NDE of damage in materials and a method to detect thermal aging degradation and plastic strain damage in duplex stainless steel.

2 DETECTION SYSTEM FOR MATERIAL DAMAGE USING SQUID

Our apparatus is shown schematically in Figure 1. It is composed of a SQUID device, a gradiometer, a superconducting magnet and a recorder.

The SQUID device is an rf(radio frequency) type. The gradiometer comprises three superconducting coils whose outer diameter is 20 mm that are series counter-wound. Such a gradiometer configuration is commonly used in SQUID applications and is known as a second-order gradiometer. Therefore, the gradiometer is sensitive only to change in field gradient $\partial^2 B/\partial z^2$. The gradiometer connects to the SQUID device through a superconducting transformer. It is able to extend dynamic sensitivity of our apparatus using the

SMiRT 11 Transactions Vol. L (August 1991) Tokyo, Japan, © 1991

Table 1 Chemical composition and ferrite content of duplex stainless steels

Material	C	Si	Mn	P	S	Cr	Ni	Mo	Co	N	Ferrite content (%)
CF3M(A)	0.016	1.36	0.16	0.014	0.005	19.4	10.05	2.21	0.03	—	12.5
CF3M(B)	0.01	1.25	0.63	0.010	0.006	20.30	9.54	2.14	0.03	0.04	21.3
CF3M(C)	0.02	1.39	0.59	0.018	0.006	20.74	9.67	2.30	0.04	0.03	26.1

transformer.

A test specimen on the moving table is magnetized by the superconduting magnet. This magnet produces a polarising field of up to 0.03 T at a distance as large as 150 mm below the gradiometer.

The SQUID sensor and superconducting magnet are within a liquid helium (4.2K) cryostat. The cryostat is made from nonmagnetic FRP material.

3 EXPERIMENTAL PROCEDURE

3.1 Materials

Materials used in this experiment are three heats of commercially duplex stainless steel that are ASTM CF3M. These chemical compositions and ferrite contents are shown in Table 1.

The duplex stainless steels were damaged two ways. One damage was thermal aging. Duplex stainless steels are known to lose toughness if aged at high temperatures (typically 748K). Therefore, test blocks of each material were aged at 748K in an electrical furnace for up to 1346 hours.Round bar test specimens (10 mm in length and 5 mm in diameter) were cut from these blocks at various aging times from 0 to 1346 hours.

The other damage was plastic strain. Round bar tensile test specimens (70 mm in gauge length and 8 mm in diameter) were cut from these virgin blocks.

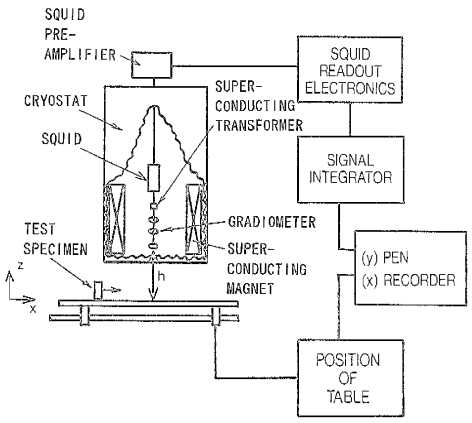

Figure 1 Schematic representation of SQUID system for NDE

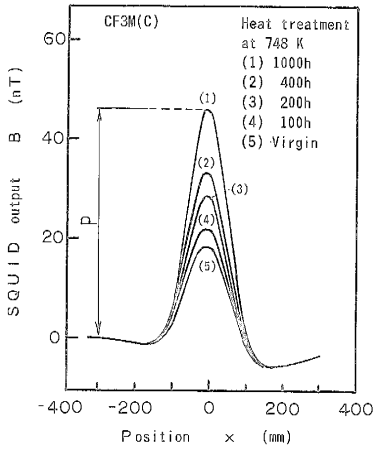

Figure 2 SQUID response for aged specimens passing beneath the cryostat

A tensile test was performed on the specimens at ambient temperature. After tensile strain up to 2%, round bar test specimens (10 mm in length and 5 mm in diameter) were cut at various plastic strains from 0 to 2%.

3.2 Test condition

The specimens were measured by passing them below the gradiometer on the moving table shown in Figure 1. The standoff distance between the gradiometer and table was about 150 mm.

The SQUID output is plotted as a function of the position of the test specimen in Figure 2. This output shows a pronounced positive peak at zero when the specimen is directly beneath the gradiometer center. The amplitude of the SQUID output (P) increased with aging time. Therefore, specimen damage was detected by remote measurements up to 150 mm away from the specimen.

4 MAGNETIC FIELD ANALYSIS

The SQUID output is influenced significantly by standoff distance, test specimen size and so on. Thus, a method to analyze the magnetic field in order to calibrate the SQUID output (P) directly by the magnetization of a test specimen is described.

The magnetic field distribution of the test specimen is like that of a bar magnet. It can be represented by two magnetic poles ($\pm m$) separated by the length of the specimen (2ℓ). This mathematical model of the specimen is shown in Figure 3. Using this model with Coulomb's law, the magnetic field (Bc) at the center of a gradiometer coil is given by:

$$Bc = \frac{m}{4\pi}\left(\frac{h-\ell}{r_1^3} - \frac{h+\ell}{r_2^3}\right) \quad \cdots\cdots (1)$$

Where; m is the magnetic pole strength
h is the standoff distance between the specimen and the gradiometer coil
r_1, r_2 are the distances from the poles to the gradiometer coil.

The second-order gradiometer is composed of three coils of 2, -4 and 2 turns. The magnetic field (Bc) linking these coils respectively can be calculated using equation (1). If these magnetic fields at each gradiometer coil were Bc_1, Bc_2 and Bc_3, the SQUID output (P) is given by:

$$P = 2(Bc_1 - 2Bc_2 + Bc_3) \quad \cdots\cdots (2)$$

In order to calculate the internal magnetic field of a test specimen, we analyzed the magnetic field distribution of a solenoid coil with the same dimension as the test specimen. The pole strength (m) of the solenoid is given by:

$$m = Ss \cdot Be \quad \cdots\cdots (3)$$

Where; Ss is the cross section of the solenoid
Be is the magnetic field at the end of the solenoid.

This definition of m as the magnetic flux through the end of the solenoid is consistent with the mathematical representation in equation (1). We assumed that the field distribution in a magnetized test specimen is like that inside the solenoid. Thus, the magnetic flux density of the test

specimen was equivalent to the center magnetic field of the solenoid Bs. The ratio Bs/Be can be calculated from the standard formula.

In order to experimentally verify the validity of this analysis method, we compared the magnetic flux density measured from the hysteresis loop with that calculated from the SQUID output. The calculated values of the magnetic flux density agreed well with the measured values as shown in Figure 4.

5 TEST RESULTS

5.1 Detection of thermal aging degradation

The magnetic flux density (Bp) of specimens calculated from the SQUID output in 0.03 T by the superconducting magnet is shown in Figure 5. Bp was independent of aging time. Additionally, Bp became larger when the specimen's ferrite content increased.

The coercive force of the specimen was obtained from the superconducting magnetic field when the SQUID output was zero while changing the magnetic field. The result of coercive force (Hc) is shown in Figure 6. Hc increased with aging time. The increasing ratio of Hc was independent of the ferrite content of CF3M.

5.2 Detection of plastic strain damage

The calculated magnetic flux density of specimens in 0.03 T by the superconducting magnet is shown in Figure 7. The magnetic flux density (Bp) in the high field increased with plastic strain. However, an increasing ratio of Bp tended to be saturated with plastic strain.

The result of coercive force is shown in Figure 8. The coercive force (Hc) of specimens was found to be independent of the plastic strain.

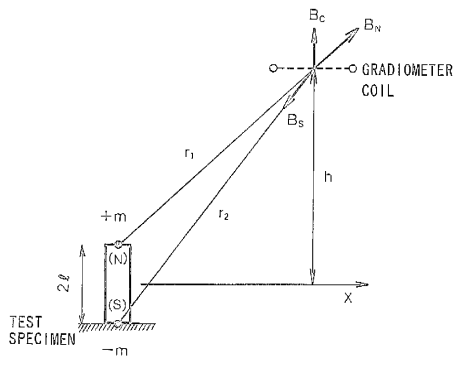

Figure 3 Mathematical model of the premagnetized test specimen

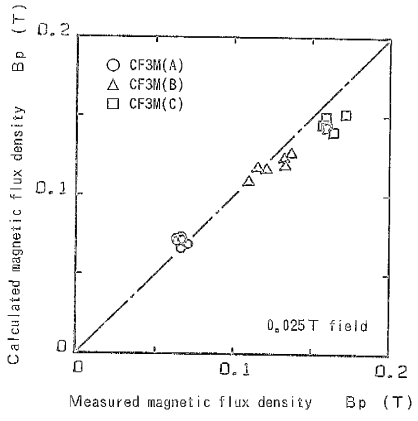

Figure 4 Comparsion of the calculated magnetic flux density from SQUID response with the measured magnetic flux density of test specimens

6 DISCUSSION

In general, it has been known that magnetization depends on the ferrite phase in cast duplex stainless steels, and that the steels cause precipitation of chromium-rich α' particles that are in a nonmagnetic phase (Chopra et al. (1985)). During the thermal aging at 748K, there is not a big ratio change of the ferrite phase in the duplex stainless steels. In the high field, much like magnetic saturation, all of the magnetic domains in the ferrite phase are arranged in the direction of the external field. Thus, the magnetic flux density of the duplex stainless steels in the high field was independent of the aging time, as shown in Figure 5. The magnetic saturation of duplex stainless steel becomes larger the more the ferrite content of the steel increases. Therefore, Bp of CF3M(C), which was the highest ferrite content among these steels, was the largest value as shown in Figure 5.

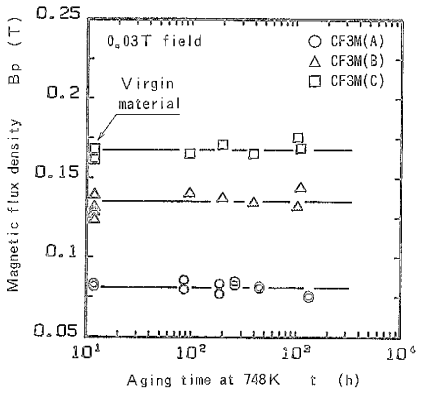

Figure 5 Magnetic flux density in the 0.03 T field plotted as a function of aging time

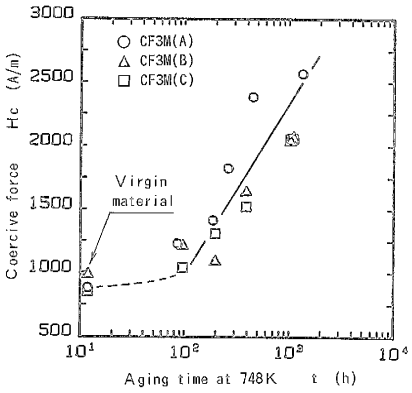

Figure 6 Coercive force plotted as a function of aging time

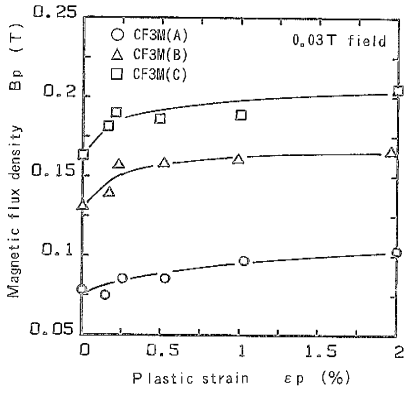

Figure 7 Magnetic flux density in the 0.03 T field plotted as a function of plastic strain

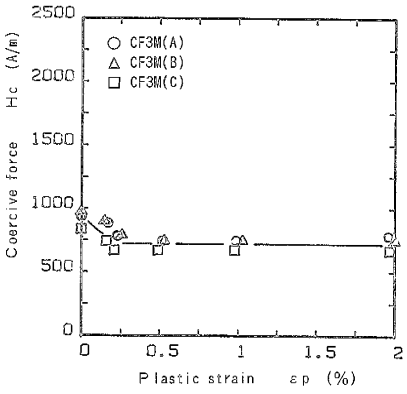

Figure 8 Coercive force plotted as a function of plastic strain

On the other hand, coercive force of the aged materials increased with the aging time, as shown in Figure 6. Fine precipitates such as α' particles deposited during the aging subdivide the magnetic domains in the ferrite phase.

Since this subdivision increases resistance to domain wall movement and domain rotation, it is assumed that the coercive force of the steels increases with precipitates of α' particles during the aging.

It is well known that the magnetic characterization of a material changes under plastic strain. This phenomenon has been explained in terms of the deformation of the magnetic domain and the magnetostriction effect. Thus, magnetic flux density of the steels in the high field increased with the plastic strain as shown in Figure 7.

However, coercive force was independent of the plastic strain as shown in Figure 8. This is because the resistance to domain wall movement and domain rotation of these steels is not affected by the plastic deformation, since the domains in the ferrite phase are subdivided by plastic deformation.

As mentioned above, in the duplex stainless steels, the magnetic flux density under the high field was found to be independent of thermal aging. Coercive force increased with thermal aging time. On the other hand, the magnetic flux density under the high field increased with the plastic strain. Coercive force was found to be independent of the plastic strain. Therefore, the degradation of thermal aging and plastic strain for duplex stainless steel were successfully detected independently using the SQUID sensor.

7 CONCLUSIONS

Detection of thermal aging and plastic strain damage for duplex stainless steels has been investgated using the SQUID sensor. The results are summarized as follows:

(1) An apparatus for nondestructive inspection was developed using a SQUID sensor. Measurements were obtained with the SQUID sensor located approximately 150 mm from the specimen.

(2) An analysis method of the magnetic field in order to calibrate the SQUID output directly to the magnetization of a test specimen was established.

(3) In the duplex stainless steels, the magnetic flux density under the high field was found to be independent of thermal aging. Coercive force increased with thermal aging time. On the other hand, the magnetic flux density under the high field increased with the plastic strain. Coercive force was found to be independent of the plastic strain. Therefore, the degradation of thermal aging and plastic strain for duplex stainless steel can be detected independently from the phenomenon.

REFERENCES

Bain,R.J., Donaldson,G.B. and Evanson,S. (1987). IEEE Trans. Magnetics, MAC-23, 473.

Bellingham,J.G., Macbicar,M.L.A. and Nisenoff,M. (1987). IEEE Trans. Magnetics, MAG-23 , 477.

Chopra,O.K. and Chung,H.M. (1985). Nucl. Eng. Des., 89 , 305.